The HI Environment of Counter-rotating Gas Hosts: Gas Accretion from Cold Gas Blobs

Aeree Chung[1]⋆, Martin Bureau[2]†, J. H. van Gorkom[3]‡, and Bärbel Koribalski[4]§

[1]*Department of Astronomy and Yonsei University Observatory, Yonsei University, Seoul 120-749, Korea*
[2]*Sub-Department of Astrophysics, University of Oxford, Denys Wilkinson Building, Keble Road, Oxford OX1 3RH, United Kingdom*
[3]*Department of Astronomy, Columbia University, 550 West 120th Street, New York, NY 10027, U.S.A.*
[4]*Australia Telescope National Facility, CSIRO, PO Box 76, Epping, NSW 1710, Australia*

Draft Version

ABSTRACT

We probe the HI properties and the gas environments of three early-type barred galaxies harbouring counter-rotating ionized gas, NGC 128, NGC 3203 and NGC 7332. Each system has one or more optically-identified galaxy, at a similar or as yet unknown redshift within a 50 kpc projected radius. Using HI synthesis imaging data, we investigate the hypothesis that the counter-rotating gas in these galaxies has been accreted from their neighbours. In NGC 128 and NGC 3203, we find 9.6×10^7 and 2.3×10^8 $M_\odot$ of HI, respectively, covering almost the entire stellar bodies of dwarf companions that appear physically connected. Both the HI morphology and kinematics are suggestive of tidal interactions. In NGC 7332, we do not find any directly-associated HI. Instead, NGC 7339, a neighbour of a comparable size at about 10 kpc, is found with 8.9×10^8 $M_\odot$ of HI gas. More recently in a single dish observation, however, another group discovered a large HI structure which seems to be an extension of NGC 7339's HI disc and also covers NGC 7332. All these observations thus suggest that HI gas is being accreted in these three galaxies from their companions, which is likely responsible for the kinematically-decoupled gas component present in their central region. In particular, the dynamical friction timescales of the nearest neighbours with HI gas of NGC 128 and NGC 3203 are comparable to their orbital timescales around the counter-rotators, several $\sim 10^8$ yr, implying that those neighbours will likely soon merge with the primary galaxies, fueling them with gas. NGC 7332 also appears to be in the merging process with its neighbour through the common HI envelope. Besides, we find some other potential gas donors around NGC 128 and NGC 7332: two HI-rich galaxies with $M_{HI} = 3.8 \times 10^8$ and 2.5×10^9 $M_\odot$ at a distance of ≈ 67 kpc from NGC 128, and two dwarf systems with $M_{HI} = 3.9 \times 10^7$ and 7.4×10^7 $M_\odot$ at $\lesssim 100$ kpc from NGC 7332. Among the seven HI features identified in this study, three of them are associated with dwarf galaxies, two of which have only been recently identified in a blind survey while the third one is still not catalogued at optical wavelengths. Considering the incompleteness of existing studies of the faint dwarf galaxy population both in the optical and in HI, accretion from cold gas blobs, presumably gas-rich dwarfs, is expected to occur even more frequently than what is inferred from such cases that have been observed to date.

Key words: ISM: kinematics and dynamics – galaxies: bulges – galaxies: evolution – galaxies: interactions – galaxies: structure

1 INTRODUCTION

Morphological and dynamical peculiarities of galaxies can be used as diagnostics of galaxy formation. Features such as tails, bridges, rings and distinct kinematic or stellar population components help us to better understand the structural parameters of galaxies and their formation mechanisms (e.g. Hernquist & Barnes 1991; Bekki 1998; Bertola et al. 1998).

⋆ E-mail:achung@yonsei.ac.kr
† E-mail:bureau@astro.ox.ac.uk
‡ E-mail:jvangork@astro.columbia.edu
§ E-mail:Baerbel.Koribalski@csiro.au

A counter-rotating gas disc during galaxy formation is dynamically unstable. Kinematically-distinct gas components are therefore more likely to be the result of subsequent accretion than of being primordial (Puerari & Pfenniger 2001). Counter-rotating gas is more common in elliptical and lenticular (S0) galaxies than gas-rich spirals (see Bureau & Chung 2006 for an extensive discussion of the frequency in S0s; Sarzi et al. 2006 and Davis et al. 2011 for ellipticals). As Kannappan & Fabricant (2001) argue, this probably reflects both that 1) it is harder for counter-rotating gas to survive in late-type galaxies due to friction within co-rotating material, and 2) the accretion event itself can help consume most of the gas in a triggered starburst, which may yield a gas-poor early-type system with some kinematically-distinct gas leftover. Hence studying the origin(s) of counter-rotating gas is important to understand the formation and evolution of galaxies, in particular that of the early-type population, and growth through gas accretion and minor mergers (Bournaud, Jog & Combes 2007; Györy & Bell 2010).

For the origin of counter-rotating gas, sporadic or continuous gas infall from the galactic halo and merging with gas-rich systems have been suggested (see Thakar & Ryden 1998, and references therein). Alternatively, gas accretions from filaments, predicted to occur frequently in low-density regions today (e.g. Kereš et al. 2005), may well form kinematically-distinct components. As some simulations have shown (e.g. Thakar & Ryden 1996), continuous gas infall might be best suited for the creation of extensive counter-rotating gas discs. Observationally, on the other hand, a number of counter-rotators with hints of minor merging events have been found (e.g. Haynes et al. 2000), although we still lack bullet-proof evidence of gas accretion directly associated with these merging events. One such *smoking gun* example is the galaxy pair NGC 1596 and NGC 1602 (Chung et al. 2006).

NGC 1596 is one of the counter-rotators serendipitously found by Chung & Bureau (2004) in the sample of Bureau & Freeman (1999). As shown in Figure 1 of Bureau & Chung (2006), the galaxy hosts ionized gas that in the central few kpc is rotating in the opposite direction to the bulk of the stars. The counter-rotating gas is kinematically asymmetric, extending up to 150 km s^{-1} on one side of the disc while it extends less than 50 km s^{-1} on the other side. There is a companion with a similar systemic velocity, NGC 1602, at distance of 20 kpc (from centre to centre). A deep optical image by Pohlen et al. (2004) revealed extended stellar envelopes around both galaxies, with no clear border in-between (see Figure 1 in Chung et al. 2006). In an HI follow-up study using the Australia Telescope Compact Array (ATCA), Chung et al. (2006) found a large HI structure covering both galaxies. The HI morphology and kinematics are quite regular with no sign of disturbance within the stellar disc of NGC 1602, while they become highly asymmetric in the outer disc. An HI tail can clearly be seen on one side, leading from NGC 1602 to the centre of NGC 1596. This strongly supports the hypothesis that much of the gas in NGC 1596 originates from its gas-rich companion and must have been heated while entering NGC 1596, as it is observed in the form of ionized gas in NGC 1596.

Besides NGC 1596, Chung & Bureau (2004) identified two more counter-rotators, NGC 128 and NGC 3203 (see also Emsellem & Arsenault 1997; Bureau & Chung 2006). As shown in Fig. 1 of Bureau & Chung (2006), the counter-rotating ionized gas in these galaxies is found to be a few kpc in size with a maximum rotation velocity comparable to the stars (≈ 150 km s^{-1}). The counter-rotating component is quite symmetric in the case of NGC 128, being widely spread to both sides of the disc, while it is mostly found on one side of the disc in NGC 3203. Both systems have closeby galaxies at similar velocities or candidate companions that are potential donors of counter-rotating gas, like NGC 1602. In this work we present results from our HI follow-up study of these galaxies, using the Very Large Array (VLA)[1] to study their HI properties and environment. In addition, we have included another well-known counter-rotator of similar morphology, the barred S0 galaxy NGC 7332 from the study of Falcón-Barroso et al. (2004).

In Section 2, we describe the general properties and the environment of our sample galaxies. In Section 3, we summarize the HI observations and data reduction. In Section 4, we describe the HI properties of the sample galaxies and their surroundings. In Section 5, we discuss the origin of the counter-rotating ionized gas and its role in galaxy evolution. We conclude in Section 6. We adopt a distance of 53.9 Mpc and 38.2 Mpc to NGC 128 and NGC 3203, respectively, based on the standard cosmology with $H_0 = 73$ km s^{-1} Mpc^{-1}, $\Omega_M = 0.27$ and $\Omega_\Lambda = 0.73$ (Spergel et al. 2003). For NGC 7332, we adopt 23 Mpc, a distance determined using the surface brightness fluctuation technique (Tonry et al. 2001), which is probably the most reliable distance for this system.

2   SAMPLE

Our sample consists of three edge-on disc galaxies, NGC 128, NGC 3203 and NGC 7332, where ionized gas ([OIII], but also Hβ for NGC 7332) has been found to rotate in the opposite direction to the stars (Emsellem & Arsenault 1997; Chung & Bureau 2004; Falcón-Barroso et al. 2004; Bureau & Chung 2006). Besides hosting kinematically-decoupled ionized gas in their centre, the galaxies in the sample have other properties in common.

Firstly, each galaxy is surrounded by several definite or potential companions. Figure 1 shows optical images of the galaxy environments. Dashed circles are drawn at 50 kpc projected radii around the counter-rotators at the adopted distance for each galaxy (angular scales of 15.3, 10.9 and 6.69 kpc per arcminute, respectively). Within 50 kpc radii, the redshifts of relatively bright neighbours (at most 15 times fainter than the counter-rotator, i.e. $\Delta m_B \lesssim 3$) are always available, and their group membership is well defined. That is, NGC 127 and NGC 130 near NGC 128, and NGC 7339 near NGC 7332, are likely true neighbours, while ESO 500-G023 in NGC 3203's field must be a background object. The redshifts of dwarf galaxies fainter than that are not available and their association with the counter-rotators remains an open question. These optically-visible
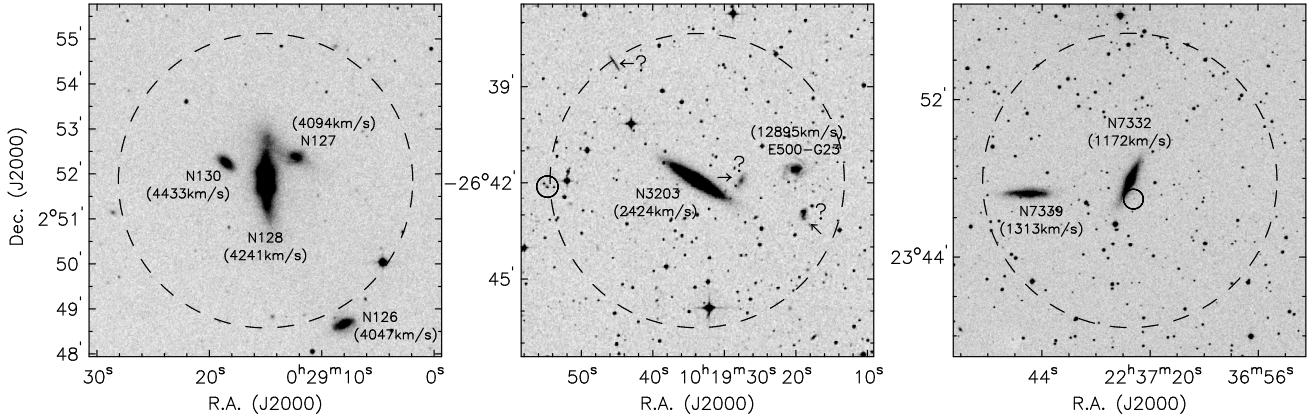

Figure 1. *B*-band optical images of the three counter-rotating gas hosts from the second Digitized Sky Survey (DSS2). From left to right: NGC 128, NGC 3203 and NGC 7332. The large dashed circles are drawn at a 50 kpc projected radius from the counter-rotators. The sample galaxies and their neighbours at <50 kpc radii with a known redshift are labeled, with the optical velocity. Small solid circles represent catalogued galaxies with no redshift within a < 50 kpc radius. All the optically-catalogued extragalactic sources (with or without a redshift) are listed in Table 1. Extended sources within this radius that are not cataloged are indicated with an arrow.

but small systems within the dashed circles (whether catalogued or not) are indicated with question marks in Figure 1. At optical wavelengths, only one galaxy among the sample, NGC 128, shows direct evidence for tidal interaction with its neighbour NGC 127, as clearly indicated by the stellar tail between them.

Secondly, all galaxies in the sample have a boxy or peanut-shaped (B/PS) bulge, which is likely the edge-on view of a thickened bar (see Bureau & Freeman 1999 and Bureau & Athanassoula 2005, and references therein). In fact, the presence of a bar has been kinematically confirmed in NGC 128 and NGC 3203 in the stellar kinematic study of Chung & Bureau (2004), and in NGC 7332 by Falcón-Barroso et al. (2004). The relevance of the counter-rotating gas and the presence of the bars will be discussed in more detail in Section 5.

The general properties of the sample galaxies and their neighbours are summarized in Table 1.

3 OBSERVATIONS & DATA REDUCTION

The VLA observations were done in 2004-5 in several configurations. NGC 128 and NGC 3203 had only H I flux upper limits at the time of observing (1.36 and 6.50 Jy km s^{-1} for NGC 128 and NGC 3203, respectively; Huchtmeier & Richter 1989) and were thus observed in D array - the most sensitive array of the VLA. NGC 3203, located in the southern sky ($\delta < -26$ deg), was also observed with the DnC hybrid configuration to obtain a better coverage of the $u - v$ plane. NGC 7332, with a prior H I flux measurement (0.84 Jy km s^{-1}; de Vaucouleurs et al. 1991, hereafter RC3), was observed in the C and DnC configurations.

Each galaxy was observed with 3.125 and 6.25 MHz bandwidths at the same time. The narrow band covers roughly 660 km s^{-1}, providing good coverage of the host galaxy, while the wide band covers > 1300 km s^{-1}, probing a broader velocity range across the sample galaxy fields. The correlators were configured to produce 127 and 63 channels with a single polarization, respectively. Online Hanning

smoothing was applied and every other channel was discarded. This resulted in 63 and 31 independent channels with a velocity resolution of 10.4 and 41.6 km s^{-1}, respectively.

The data reduction was done using the Astronomical Imaging Processing System (AIPS). Data from different configurations and bandwidths were calibrated separately. For NGC 3203 and NGC 7332, the visibility data of different baselines were merged using the AIPS command DBCON after flux, phase and bandpass calibration, while the data with different velocity resolutions were treated separately. The continuum was subtracted using a linear fit to the $u - v$ data of line-free channels at both sides of the band. Larger ranges were used for the 6.25 MHz bandwidth data. High $u - v$ points caused by interference were flagged after continuum subtraction. We first made cubes of a large field of view with a range of weighting, to search for H I emission from sources far away from the field centre. The final cubes were then made using ROBUST=1 (Briggs 1995) to maximize sensitivity while keeping a good spatial resolution.

The total H I images were made by taking moments along the frequency axis (0th moments). The task MOMNT creates a mask to blank the images at a given cutoff level. In creating the masks, we applied Gaussian and Hanning smoothing spatially and spectrally, respectively, to maximize the signal-to-noise.

Two sets of cleaned cubes per object were produced, one set for the narrow band data and one for the wide band. For each galaxy, the two sets were inspected separately and only the set showing the H I features better is presented in this paper: 6.25 MHz data for NGC 128 and 3.125 MHz data for NGC 3203 and NGC 7332. The VLA observing parameters, the spectral and spatial resolutions, and the rms of the final cubes used to produce the H I maps presented in this work are summarized in Table 2. The total H I mass in solar unit has been calculated using the formula $M_{\rm HI} = 2.356 \times 10^5 D_{\rm Mpc}^2 S_{\rm HI}$, where $D_{\rm Mpc}$ is the distance to the galaxy in Mpc and $S_{\rm HI}$ is the total H I flux in Jy km s^{-1}. All H I fluxes and hence H I masses have been corrected for the primary beam response.

Table 1. General properties and environment of the sample galaxies[a].

	NGC 128	NGC 3203	NGC 7332
Coordinate:			
α_{2000} (^{h} ^{m} ^{s})	00 29 15.0	10 19 34.5	22 37 24.5
δ_{2000} ($^\circ$ $'$ $''$)	02 51 55.0	-26 41 53.0	23 47 52.0
Morphology	S0 pec sp	SA(r)0+? sp	S0 pec sp
D_{25} (arcmin)[b]	3.0	2.9	4.1
B_T (mag)[c]	12.77	13.10	12.02
V_{opt} (km s^{-1})[d]	4241	2394	1172
Neighbours[e]	—— Object name (Δd in arcmin, ΔV_{opt} in km s^{-1}) ——		
	N127 (0.8, -147)	J10195473[f] (4.7, N/A)	N7339 (5.2, 141)
	N130 (1.0, 192)		J22372366[f] (1.0, N/A)

[a] The information about the three sample galaxies has been obtained from the Third Reference Catalog of Bright Galaxies (RC3; de Vaucouleurs et al. 1991), while the data on their neighbours have been collected from the NASA/IPAC Extragalactic Database (NED; http://nedwww.ipac.caltech.edu/).
[b] Mean apparent major isophotal diameter, measured at or reduced to the surface brightness level $\mu_B = 25.0$ B mag arcsec^{-2}.
[c] Total (asymptotic) magnitude in B, derived by extrapolation from photoelectric aperture and surface photometry with photoelectric zero point data.
[d] Mean heliocentric radial velocity, derived from optical observations.
[e] Optically identified neighbours within a 50 kpc projected radius and $\Delta V_{opt} \lesssim 1000$ km s^{-1} or no redshift. Δd is the projected distance.
[f] 2 Micron All Sky Survey (2MASS; Skrutskie et al. 2006).

Table 2. VLA observing parameters.

	NGC 128	NGC 3203	NGC 7332
Phase centre:			
α_{2000} (^{h} ^{m} ^{s})	00 29 15.1	10 19 34.4	22 37 35.9
δ_{2000} ($^\circ$ $'$ $''$)	02 51 50.0	-26 41 54.0	23 47 32.0
Configurations	D	DnC, D	C, DnC
Velocity centre (km s^{-1})[a]	4241	2409	1375
Bandwidth (MHz)	6.25	3.125	3.125
Channel width (km s^{-1})	41.6	10.4	10.4
Synthesized beam FWHM ($''$)	56.9×50.3	48.7×35.6[b]	18.8×16.5[b]
Noise (1σ)[c]:			
in mJy beam^{-1}	0.28	0.60	0.33
in 10^{19} cm^{-2}	0.45	0.40	1.23

[a] Heliocentric velocity using optical definition.
[b] Combined data from all configurations.
[c] Rms of the combined cube per channel. See text for further details.

Table 3. Summary of the H I structures.

Field	Object	H I Peak Position (^{h} ^{m} ^{s}) ($^\circ$ $'$ $''$)	V_{HI} (km s^{-1})	S_{HI}[a] (Jy km s^{-1})	log ($M_{HI}/M_\odot$)[b]	B_T[c] (mag)	M_{HI}/L_B ($M_\odot/L_\odot$)
NGC 128	UGC 298	00 29 51.315 +02 56 50.56	3930	0.56	8.58	16.01	0.25
	NGC 127	00 29 13.765 +02 52 20.60	4050	0.14	7.98	15.33	0.03[d]
	PGC 001760	00 28 37.717 +02 57 10.56	4500	3.58	9.40	15.93	1.27
NGC 3203	AC dwarf I[e]	10 19 26.984 −26 42 03.36	2560	0.66	8.36	15.86	0.22
NGC 7332	SDSS J223829	22 38 29.456 +23 51 30.80	1410	0.32	7.59	16.94	0.29
	NGC 7339	22 37 48.308 +23 48 11.97	1300	7.11	8.95	13.10	0.19
	SDSS J223627	22 36 27.737 +23 43 00.44	1400	0.59	7.87	15.74	0.18

[a] All H I fluxes have been corrected for the primary beam response.
[b] Log of H I mass in $M_\odot$ calculated adopting a distance of 53.9, 38.2 and 23.0 Mpc for the first three galaxies, AC dwarf I, and the last three galaxies, respectively. The distance to NGC 7332 is taken from the surface brightness fluctuation measurements by Tonry et al. (2001).
[c] Extracted by Paturel et al. (2000) from the Digitized Sky Survey (DSS). For galaxies not catalogued by Paturel et al. (2000), we determined the total B magnitude from the DSS image.
[d] It is assumed that the H I is associated only with NGC 127.
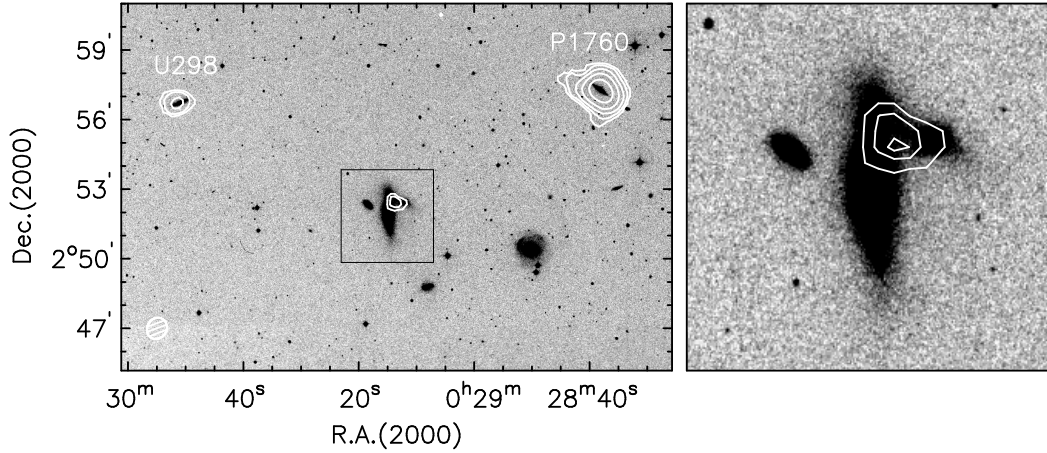[e] Object never been catalogued at any wavelength before, hence it is named temporarily in this study.

Figure 2. On the left, the H I distributions of NGC 128 and its surrounding are shown in white contours, overlaid on a grayscale optical blue image from second Digital Sky Survey DSS2. The H I contours are 2, 4, 8, ..., $\times 10^{19}$ cm^{-2}. The synthesized beam is shown at the bottom left. The H I gas to the northeast of NGC 128, that is likely bound to UGC 298, appears to be disturbed, although no direct evidence of interaction with NGC 128 is found. The H I to the northwest of NGC 128, that nicely coincides with PGC 001760, also does not show any sign of interaction. The outlined region of $4' \times 4'$ around NGC 128 is magnified on the right. The contours are drawn at H I column densities of 2, 4 and 6×10^{19} cm^{-2}. Some H I gas is found to extend over the two galaxies NGC 127 and NGC 128 (a centre to centre projected distance of ≈ 15 kpc). The H I morphology is irregular, with the peak flux between the two galaxies. The H I line profiles are presented in Figure 3.
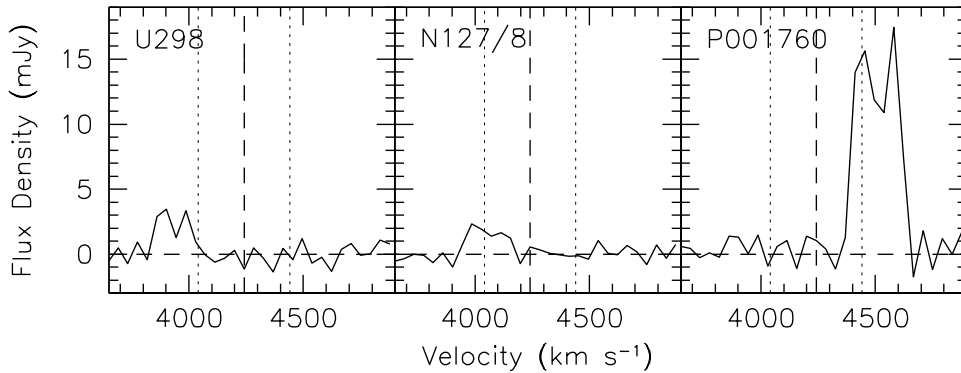

Figure 3. Total line profiles of the H I structures found in NGC 128's field. The dashed line in each panel represents the optical velocity of NGC 128; the velocity range covered by NGC 128's rotation ($V_{\rm rot} \approx 200$ km s^{-1}) is indicated by the dotted lines (Chung & Bureau 2004). The H I gas found to the northeast coincides well with UGC 298 and is likely to be associated with it, although no prior redshift measurement is available. The velocity of the H I gas to the northwest of the field coincides well with the optical redshift of PGC 001760. The H I gas found between NGC 127 and NGC 128 is spatially offset from both galaxies, although its velocity range is close to the optical velocity of NGC 127 (4094 km s^{-1}). This H I gas is likely to have been originally bound to NGC 127 and is now being transferred to NGC 128.

4 RESULTS

4.1 NGC 128

We find 9.6×10^7 $M_\odot$ of H I associated with the stellar disc of NGC 128. As shown on the right panel of Figure 2, the H I is found only on one half of the disc, covering almost the entire stellar disc of its neighbour, NGC 127. The H I spatial extent is ≈ 1 arcmin, roughly 15 kpc at this distance. Although the peak intensity occurs between the two galaxies, it is closer to the systemic velocity of NGC 127 (4094 km s^{-1}, see Fig. 3). The H I morphology and the velocity profile strongly suggest that the H I was originally bound to NGC 127 rather than NGC 128. In fact, the H I feature is also seen in the Arecibo observations of Bieging & Biermann (1977). Their spectrum is comparable to that of the VLA in its peak intensity and

velocity width. However, these authors did not make the connection with NGC 127.

We find two other H I structures in this field, both nicely coinciding with optically catalogued galaxies: UGC 298 and PGC 001760, as shown on the left panel of Figure 2. There is no optical redshift measurement for UGC 298 to date, so the velocity from our H I study is the first. Adopting the same distance as NGC 128, the H I mass of UGC 298 is 3.8×10^8 $M_\odot$. The redshift of PGC 001760 measured with our data is consistent with its optical redshift (4427±50 km s^{-1}; RC3). Adopting the same distance as NGC 128, the H I mass of PGC 001760 is 2.5×10^9 $M_\odot$. The total H I line profile of the three H I structures found in the NGC 128 field are shown in Figure 3 on the same scale.
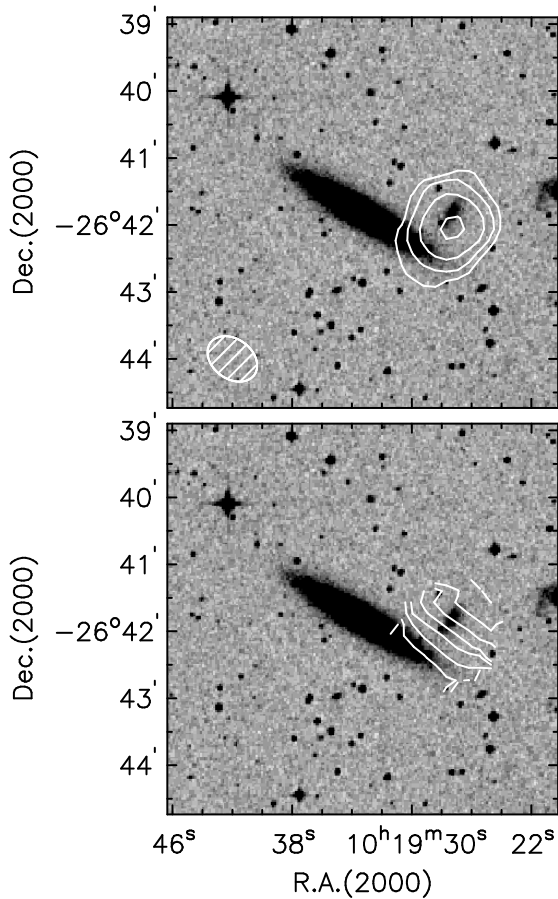
Figure 5. Total H I line profile of the gas structure shown in Figure 4 (AC dwarf I). The dashed line represents the optical velocity of NGC 3203; the dotted lines indicate the rotational velocity range ($\approx$ 180 km s^{-1}), taken from Chung & Bureau (2004). The $> 3\sigma$ feature close to NGC 3203's systemic velocity is suggestive of gas being transferred from the dwarf to NGC 3203. The H I cloud also morphologically appears to be more extended toward NGC 3203's disc, as seen in Figure 4.

NGC 3203. As shown in Figure 5, the H I cloud velocity is found well within the range of velocities covered by the disc of NGC 3203 (2424 $\pm$ 150 km s^{-1}; Chung & Bureau 2004). This makes the connection of the H I cloud and the counter-rotating ionized gas in NGC 3203 even more likely. The off-set between the H I peak and the optical centre of the dwarf could well be an indication of the tidal interaction between the two galaxies.

We do not find any other H I gas in this field and name the newly discovered H I-rich dwarf "AC dwarf I".

4.3 NGC 7332

We find 8.9×10^8 $M_\odot$ of H I in NGC 7332's neighbour, NGC 7339, while we do not find any H I gas directly associated with NGC 7332 itself. Note, however, that the prior H I detection of NGC 7332 by Knapp, Kerr & Williams (1978), which was incorporated into the RC3 is likely to have come from Arecibo side-lobes picking up NGC 7339 as already suggested by others such as Haynes (1981). The optical centres of the two galaxies are $\approx$ 30 kpc apart, but the closest projected distance that can be measured is only $\approx$16 kpc at the distance of the pair, as measured from the DSS2 image down to the survey surface brightness limit.

Morganti et al. (2006) reported an H I cloud of 6 $\times$ 10^6 $M_\odot$ at a redshift of 1250 km s^{-1} from WSRT data, almost halfway spatially between the two galaxies. To confirm this, we have tapered our VLA data to $31'' \times 29''$, a beam similar to that of the WSRT ($41'' \times 30''$), and Hanning smoothed the cube to 15 km s^{-1}, a comparable velocity resolution to that of the WSRT cube (16 km s^{-1}). We present in Figure 6 the H I image obtained from the smoothed and tapered cube using the same contour levels as those of Morganti et al. (2006). Although our 3σ H I mass sensitivity in this cube is 1.2×10^6 $M_\odot$, we do not detect the 6×10^6 $M_\odot$ H I cloud seen by Morganti et al. (2006).

Figure 4. Top: H I distribution of NGC 3203 and its surroundings, shown in white contours on top of the DSS2 blue image. The synthesized beam is shown at the bottom left. The H I contours are 3, 6, 12 and 24$\times10^{19}$ cm^{-2}. An H I-rich dwarf galaxy is found near NGC 3203, not catalogued at any wavelength yet. Although the peak of the H I gas is slightly offset from the optical centre of the dwarf ($\approx 6''$ or 1 kpc), the optical and H I emission more or less coincide on the sky, with almost the same major axis (perpendicular to NGC 3203's disc). Bottom: H I velocity field. Starting from the contour crossing NGC 3203's disc, the velocity contours are 2520, 2530, 2540, ..., and 2580 km s^{-1}. It is clearly seen that the iso-velocity contours are almost prependicular to the major axis of the dwarf companion. This strongly suggests that the H I cloud is rotationally supported and bound to the dwarf.

4.2 NGC 3203

We find an H I blob toward the southwest edge of NGC 3203's optical disc. The H I gas mass is 2.3×10^8 $M_\odot$ at the distance of NGC 3203. As shown in Figure 4, there is a dwarf galaxy at the position of this H I cloud, and the closest projected distance that can be measured between the two galaxies (from edge to edge) is about 2.5 kpc. This small *disky* galaxy had not been optically-identified to date, and hence its redshift is not available in any database. Although the centre of the H I cloud and the optical centre of the dwarf are offset by $\approx$ 1 kpc (assuming the same distance as NGC 3203), they are largely coincident and the H I cloud is elongated in the same direction as the major axis of the dwarf (almost perpendicular to NGC 3203's disc). This is highly suggestive that the origin of the H I cloud is the dwarf rather than
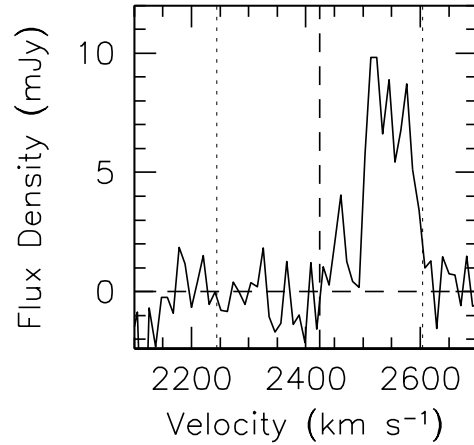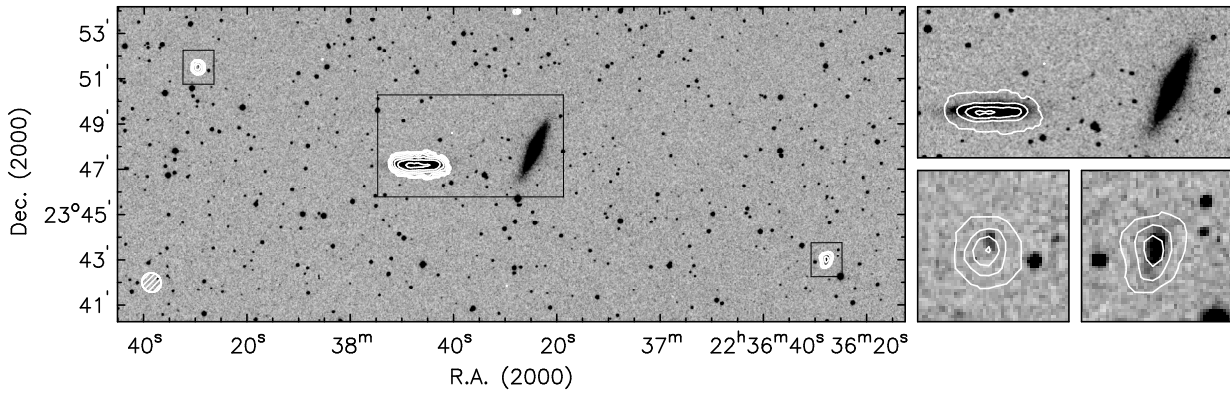
Figure 6. On the left, the H I found in NGC 7332's field is shown in white contours overlaid on the DSS2 blue image. This H I image was produced using the data cube smoothed to a beam of $31'' \times 29''$ and a velocity resolution of 15 km s^{-1}, comparable to those of Morganti et al.'s (2006) WSRT data. The contours correspond to H I column densities of 1, 2.5, 5, 10, 25, ...$\times 10^{19}$ cm^{-2}. The smoothed synthesized beam is shown at the bottom left. The regions outlined with boxes are magnified on the right. On the top right, the pair NGC 7332 (right) and NGC 7339 (left) is magnified ($9' \times 4.5'$). The contours of the H I gas are the same as the figure on the left side. On the bottom right, $2.5' \times 2.5'$ areas around the peaks of the two small H I structures are shown, again with the same contours. These two galaxies are catalogued in the Sloan Digital Sky Survey (SDSS) but no optical spectrum is available, and hence the optical redshifts are not known.
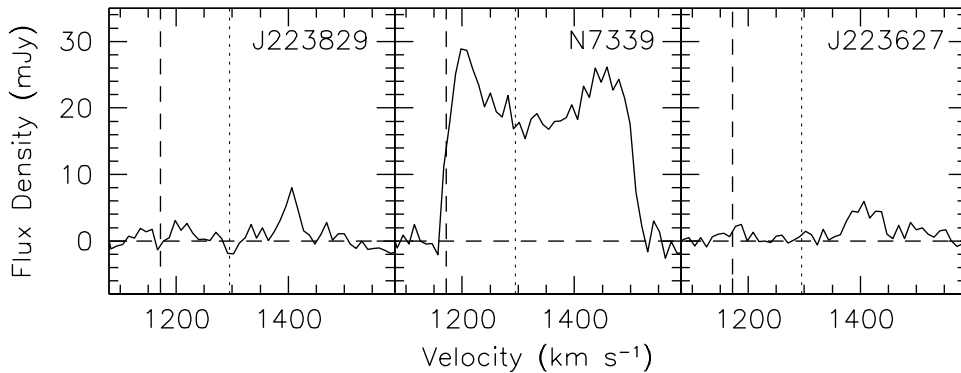

Figure 7. Total H I line profiles of the gas structures shown in Figure 6. The dashed line represents the optical velocity of NGC 7332; the dotted lines represent its rotational velocity range (≈ 250 km s^{-1}), taken from Falcón-Barroso et al. (2004).

More recently, Minchin et al. (2010) have discovered a large H I structure covering both NGC 7339 and NGC 7332, with the H I peak coinciding with the center of NGC 7339. As shown in their H I image and renzogram (their Figs. 8 and 10), this large H I envelope appears to be an extension of NGC 7339's H I disc. Morganti et al. (2006)'s cloud could well be the part of this feature, and it is possible that they detected one of the high density regions. Indeed, the total VLA H I flux is $\approx$20% lower than the single-dish flux of Minchin et al. (2010), and it is likely that we are missing some diffuse H I.

We also find two other H I clouds in the cube at a similar redshift ($\approx$1400 km s^{-1}), as shown in Figures 6 and 7. These two H I structures coincide with dwarf galaxies identified in the Sloan Digital Sky Survey (SDSS) (Fig. 8), but their optical redshifts are unknown. At the location of the H I structure to the southwest of NGC 7332, there is only one possible optical counterpart, J223627.84+234257.5, while there are two candidates at the location of the northeast H I structure, under a single catalogue number, J223829.69+235131.2. Based on its colour and fuzziness, the blue object is more likely to be the true counterpart of the H I gas. The red object shows

no substructure but a similar colour as other faint stars in the field, hence it is probably a faint foreground star. In fact, the H I peak coincides better with the optical centre of the blue galaxy. The two H I-rich galaxies are located almost at the half power point at the primary beam and their H I fluxes measured after primary beam correction are consistent within the errors with those of Minchin et al. (2010). The H I masses are about 3.9×10^7 $M_\odot$ and 7.4×10^7 $M_\odot$, respectively.

Unlike for NGC 128 and NGC 3203, we do not find any direct evidence for interaction between NGC 7332 and its neighbours, NGC 7339 and the two H I-rich dwarfs. However, the H I gas morphology and kinematics found by Minchin et al. (2010) are highly suggestive that NGC 7332 and NGC 7339 are tidally affecting each other, even considering the large beam of the single dish. It is also noteworthy that NGC 7332 is in a gas rich environment, with several potential gas donors.

5   DISCUSSION

5.1   The origin of counter-rotating gas

In this H I follow-up study, we have found H I gas in the disc of two out of the three galaxies hosting kinematically-decoupled ionized gas observed. In both cases, the H I gas is highly offset from the optical centre of the counter-rotator, being found only on one side of the disc. In addition, in both cases, the H I gas covers a large fraction of a dwarf companion. In the case of NGC 127, the companion of NGC 128, the H I covers most of its stellar body, although it is spatially offset and more extended toward NGC 128, filling up the intergalactic space between the pair where diffuse light (likely tidally-stripped stars) is present. The centre of the H I velocity coincides well with the optical systemic velocity of NGC 127, and the entire H I velocity range is well within the range covered by NGC 128's rotational velocity. In the case of the dwarf companion of NGC 3203, AC dwarf I, the H I covers its entire stellar body. AC dwarf I appears to be disky, and the H I cloud is enlongated in the same direction as its disc, the major axis being perpendicular to that of NGC 3203. The H I velocity range overlaps with the rotational velocity range of NGC 3203 by a few tens of km s^{-1}.

These observations strongly suggest gas accretion onto NGC 128 from NGC 127, and onto NGC 3203 from AC dwarf I. The counter-rotating ionized gas present in NGC 128 and NGC 3203 (see Fig. 1 of Bureau & Chung 2006) is thus likely to originate from this externally accreted gas. As the ISM from the dwarf neighbours enters in retrograde motion with respect to the stellar discs, it must be shock-heated and is (partially) currently observed in the form of ionized gas.

In NGC 7332, we have not found any H I gas directly associated with the disc in our VLA observations. Minchin et al. (2010) however find a large scale H I envelope centered on its neighbour, NGC 7339, that extends all the way to NGC 7332, and it covers its entire stellar disc. In addition, both the H I and the optical morphologies show an asymmetry in the outer disc while the inner disc appears quite symmetric. Our high resolution VLA data reveal a short tail pointing to the north east and the stellar envelope is more extended and thicker on the west side, NGC toward NGC 7332.

These facts strongly suggest a tidal interaction between NGC 7332 and NGC 7339. If the H I in NGC 7339 was more extended than the stellar disk, as is often seen in spirals, then a tidal interaction would have stripped the gas before the stars are pulled out. The stripped gas would likely have fallen toward the center of NGC 7332, forming the counter-rotating gas in its centre. This is also supported by the kinematics of the counter-rotating ionized gas observed by Falcón-Barroso et al. (2004), which is tilted with respect to the equatorial plane in the direction of NGC 7339.

5.2   The fate of companions

The time required for a companion to spiral into the primary galaxy can be characterized by the dynamical friction timescale (Binney & Tremaine 1987),

$$t_{\rm fric} = \frac{1.17}{\ln\Lambda} \frac{r_{\rm i}^2 v_{\rm c}}{GM}, \qquad (1)$$
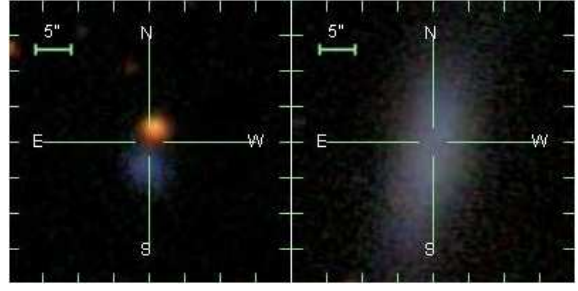

Figure 8. Sloan Digital Sky Survey (SDSS) Data Release (DR) 7 colour images of the two small H I-rich galaxies in NGC 7332's field. The H I peak of J223829 in Figure 7 coincides well with the optical peak of the blue object shown on the left. The red object is likely to be a foreground star.

where $r_{\rm i}$ is the initial radius of the orbit, $v_{\rm c}$ is the orbital velocity, G is the gravitational constant, M is the mass of the companion, and $\ln\Lambda$ is the Coulomb logarithm. As described in Binney & Tremaine (1987), the appropriate Λ can be approximated by $r_{\rm i}v_{\rm c}^2/GM$ for this case. In more practical units, this relation can be rewritten as

$$\frac{t_{\rm fric}}{\rm yr} \approx \frac{2.26 \times 10^{14}}{\ln\Lambda} \left(\frac{r_{\rm i}}{\rm kpc}\right)^2 \left(\frac{v_{\rm c}}{\rm km\ s^{-1}}\right) \left(\frac{M}{M_\odot}\right)^{-1}. \qquad (2)$$

We adopt the projected distance from the primary galaxy to its companion ($d_{\rm sep}$) and their velocity difference (ΔV) as the orbital radius $r_{\rm i}$ and velocity $v_{\rm c}$, respectively. The same line-of-sight distances as the sample galaxies have been assumed. Companion masses have been estimated using the disc size ($R_{\rm disc}$) and the H I linewidth measured at 20% of the peak flux $W_{\rm HI}$, assuming that the companions are rotationally supported ($M_{\rm comp} \approx V_{\rm rot}^2 R_{\rm disc}/G$, where $V_{\rm rot} \equiv W_{\rm HI}/2$). The disc size has been estimated from the H I extent except for NGC 127 which has a larger stellar disc compared to its H I disc. The dynamical friction and orbital timescales of the neighbours found with H I gas are compared in Table 4.

The orbital period around the galaxy hosting counter-rotating gas has been estimated for each neighbour by $t_{\rm orbit} \approx 2\pi d_{\rm sep}/\Delta V$. For NGC 128 and NGC 3203, $t_{\rm fric}$ and $t_{\rm orbit}$ of their nearest companions are comparable and of the order of 10^8 yr. This implies that these pairs are likely to soon merge and form a single system, fueling the primary galaxies with $10^7 - 10^8$ $M_\odot$ of H I gas. In fact, the H I discs of NGC 127 and AC Dwarf I appear to cover some of their primary galaxy's discs already. This strongly supports the hypothesis that these two neighbours have been feeding NGC 128 and NGC 3203 with gas. For UGC 001760, $t_{\rm fric}$ and $t_{\rm orbit}$ are comparable but it is expected to take much longer than 10^9 yr to merge with NGC 128, while it will take even longer for UGC 298 to spiral into NGC 128.

The estimated Coulomb logarithm of NGC 7339 is negative (i.e. $v_c^2/r_i < GM/r_i^2$), suggesting that this galaxy is already in the process of merging with NGC 7332. This is also supported by the observations of Minchin et al. (2010). We also have estimated $t_{\rm fric}$ and $t_{\rm orbit}$ for the two farther dwarf neighbours, using W_{20} and assuming that they are rotationally supported. For these two dwarfs, $t_{\rm fric}$ measured using the H I extent is about an order of magnitude larger than $t_{\rm orbit}$, and it may take many orbital periods for these

Table 4. Dynamical timescales for the neighbours.

Field	Companion	$V_{\rm rot}$[a] (km s^{-1})	$R_{\rm disc}$[b] (kpc)	$M_{\rm comp}$[c] ($10^9\ M_\odot$)	$d_{\rm sep}$[d] (kpc)	ΔV (km s^{-1})	$t_{\rm fric}$ (10^9 yr)	$t_{\rm orbit}$ (10^9 yr)
NGC 128	UGC 298	107	12	31.7	162	399	12.0	3.3
	NGC 127	125	11	39.8	12	150	0.3	0.5
	PGC 001760	134	20	83.0	162	300	5.8	3.3
NGC 3203	AC Dwarf I	47	11	4.9	14	150	0.5	0.5
NGC 7332	J223829	37	5	1.6	102	225	49.3	2.8
	NGC 7339	172	22	151.4	31	140	-2.7	1.4
	J223627	37	5	1.6	92	230	41.3	2.5

[a] Disc rotational velocities of companions estimated using $W_{\rm HI}/2$. The inclination w.r.t. the observer's line-of-sight has not been taken into account, hence our estimations are lower limits for $V_{\rm rot}$.
[b] The disc size has been measured using the HI extent, except for NGC 127 which is larger in the optical. The same distance as their primary galaxies have been adopted.
[c] Dynamical masses of companions calculated using $V_{\rm rot}$ and $R_{\rm disc}$ assuming a rotationally supported disc and spherical symmetry, i.e. $M_{\rm comp} = V_{\rm rot}^2 R_{\rm disc}/G$.
[d] Separations of the pair centers.

two dwarf galaxies to merge. As they approach NGC 7332 and 7339, however, it is still possible that diffuse gas outside their stellar body at large radii could be stripped by the halo of their bigger neighbours, also fueling the pair (as suggested by Grcevich & Putman 2009, for satellites of the Milky Way).

5.3 Incidence of gas counter-rotation and frequency of accretion from cold gas blobs

The fraction of all S0 galaxies with ionized gas counter-rotation is found to be some 15 per cent and slightly increases ($\approx$ 23 per cent) for galaxies with detected ionized gas only (Bureau & Chung 2006, and references therein). This provides a lower limit to the gas accretion frequency among lenticular galaxies. This fraction however does not include 1) the elliptical galaxy population and 2) gas accreted in prograde orbit. Taking these into account, the inferred frequency of gas accretion in early-type galaxies overall is expected to increase. This is supported by the high HI detection rate found by Morganti et al. (2006, see also Oosterloo et al. 2010) in their carefully selected E/S0 galaxies, many of which show direct evidence or hints of interaction. All these facts suggest that gas accretion from cold gas blobs is common among E/S0s, and is thus an important source for their continous build-up.

In gas-rich late-type galaxies, where the gas acquired from outside (either prograde or retrograde) is likely to be swept away by existing gas on relatively short timescales, evidence of gas accretion (especially from small gas blobs) may not be detected as frequently as in the E/S0 population (Bureau & Chung 2006). Assuming the same statistics as for early-type galaxies, however, merging of small gas-rich dwarfs is also expected to be common among gas-rich late-type galaxies, and also may play an important role in replenishing their discs.

5.4 Gas accretion and galaxy evolution

It is worth noting that all three counter-rotators targeted here are gas-poor, barred S0 systems. It is unclear, however, whether gas accretion has played any role in exhausting the

original gas in the host galaxy (e.g. by triggering a burst of star formation) or whether gas counter-rotation is preferentially observed in early-type systems simply because retrograde gas accretion can last longer than in gas-rich galaxies (where it is likely to be swept away by co-rotating gas; see Wardle & Knapp 1986; Bureau & Chung 2006).

In the former case, the recent star formation rate is expected to be quite high, assuming spirals with normal gas contents are the ancestors of the hosts. As discussed in detail in the previous sections, the time the nearest neighbours will take to merge into the hosts is of order a few 10^8 yrs. Assuming a L^* host with $M_{\rm gas} \approx 5 \times 10^9\ M_\odot$, our estimated dynamical friction timescales imply that these counter-rotators should have been forming stars at a rate of 5–50 $M_\odot$ yr^{-1} to use up their original gas. We however do not find any signature of such high star formation rates in the sample hosts, based on their low infrared fluxes and ionized gas emission (Knapp et al. 1989; Bureau & Freeman 1999; Chung & Bureau 2004). In addition, it is unlikely that only the gas in the host galaxies would be exhausted but not the gas in their companions, particularly in cases like NGC 127 and AC dwarf I, where we are witnessing the gas being captured by the primary galaxies.

Hence we conclude that gas accretion (and the subsequent starburst) is not likely to be responsible for the early-type morphology of our counter-rotators. It is however still possible that tidal interactions, along with gas accretion, played a role in forming the bar and bulge in these galaxies by 1) inducing instability in the disc, then 2) feeding the centre with the accreted gas, possibly triggering a nuclear starburst in some cases (e.g. Combes & Elmegreen 1993).

6 CONCLUSION

In this HI follow-up study of three galaxies where ionized gas was found to be rotating in the opposite direction to the stars in the central few kpc, we systematically find evidence for cold gas accretion from neighbours, likely to be the origin of the counter-rotating ionized gas. The dynamical friction timescales of the neighbours are short and comparable to their orbital periods around the counter-rotators,

suggesting that the pairs will merge and form a single system within about a gigayear, fueling the primary galaxy with $10^7 - 10^8$ $M_\odot$ of Hɪ. We do not find strong evidence that gas accretion is directly responsible for the early-type morphology of the sample hosts, i.e. the transformation from gas-rich spirals to gas-poor lenticular systems. However, it could well have helped to form and fuel the bar in these galaxies.

Our data, along with statistics from the literature (e.g. Bureau & Chung 2006), suggest that the accretion of cold gas blobs is an important source of gas in galaxies, and hence helps them continue to grow. Although the accretion of gas blobs is expected to be more easily detected in gas-poor early-type systems, assuming the same frequency for late-type galaxies implies that cold accretion can also play a significant role in replenishing the disc of spirals.

REFERENCES

Bekki K., 1998, ApJ, 502, L133
Bertola F., Cappellari M., Funes J. G., Corsini E. M., Pizzella A., Vega Beltrán J. C., 1998, ApJ, 509, 93L
Bieging J. H., Biermann P., 1977, MNRAS, 60, 361
Binney J., Tremaine S., 1987, Galactic Dynamics (Princeton: Princeton Univ. Press)
Bournaud F., Jog C. J., Combes F., 2007, A&A, 476, 1179
Briggs D. S., 1995, PhD Thesis, New Mexico Institute of Mining and Technology, Socorro, NM
Bureau M., Freeman K. C., 1999, AJ, 118, 126
Bureau M., Athanassoula E., 2005, ApJ, 626, 159
Bureau M., Chung A., 2006, MNRAS, 366, 182
Chung A., Bureau M., 2004, AJ, 127, 3192
Chung A., Koribalski B., Bureau M., van Gorkom J., 2006, MNRAS, 370, 1565
Combes F., Elmegreen B. G., 1993, A&A, 271, 391
Davis, T. A., et al., 2011, MNRAS, 414, 968
de Vaucouleurs G., de Vaucouleurs A., Corwin H. G., Jr., Buta R. J., Paturel G., Fouqué P., 1991 Third Reference Catalogue of Bright Galaxies (New York, Heidelberg: Springer-Verlag)
Emsellem E., Arsenault R., 1997 A&A, 318, 39L
Falcón-Barroso J., et al., 2004, MNRAS, 350, 35

Györy Z., Bell E. F., 2010, ApJ, 724, 694
Grcevich J., Putman M. E., 2009, ApJ, 696, 385
Kannappan S. J., Fabricant D. G., 2001, ApJ, 121, 140
Kereš D., Katz N., Weinburg D. H., Davé R., 2006, MNRAS, 363, 2
Knapp G. R., Kerr, F. J., Williams, B. A. 1978, ApJ, 222, 800
Knapp G. R., Guhathakurta P., Kim D.-W., Jura M. A., 1989, ApJS, 70, 329
Haynes M. P. 1981, AJ, 86, 1126
Haynes M. P., Jore K. P., Barrett E. A., Broeils A. H., Murray B. M., 2000, AJ, 120, 703
Hernquist L., Barnes J., 1991, Nature, 354, 210
Huchtmeier W. K., Richter O.-G., 1989, A General Catalog of Hɪ Observations of Galaxies (New York, Heidelberg: Springer-Verlag)
Minchin R. F., et. al., 2010, AJ, 140, 1093
Morganti R., et al., 2006, MNRAS, 371, 157
Oosterloo T., et al., 2010, MNRAS, 409, 500
Paturel G., Fang Y., Petit C., Garnier R., Rousseau J., 2000, A&AS, 146, 19
Pohlen M., Bacells M., Lütticke R., Dettmar R.-J, 2004, A&A, 422, 465
Puerari I., Pfenniger D., 2001, Ap&SS, 276, 909
Sarzi M., et al., 2006, MNRAS, 366, 1151
Skrutskie M. F., et al., 2006, AJ, 131, 1163
Spergel D. N., et al., 2003, ApJS, 148, 175
Thakar A. R., Rydden B. S., 1996, ApJ, 461, 55
Thakar A. R., Rydden B. S., 1998, ApJ, 506, 93
Tonry J. L., Dressler A., Blakeslee J. P., Ajhar E. A., Fletcher A. B. Luppino G. A., Metzger M. R., Moore C. B., 2001, ApJ, 546, 681
Wardle M, Knapp, G. R., 1986, AJ, 91, 23